Anti-proliferative Activity of 2,6-Dichloro-9- or 7-(Ethoxycarbonylmethyl)-9*H*-or 7*H*-Purines against Several Human Solid Tumour Cell Lines

Fátima Morales,[a,1] Alberto Ramirez,[b,c,1] Ana Conejo-García,[a] Cynthia Morata,[b] Juan A. Marchal,[b] Joaquín M. Campos,[a,*]

[a]*Departamento de Química Farmacéutica y Orgánica, Facultad de Farmacia, c/ Campus de Cartuja s/n, 18071 Granada (Spain).*

[b]*Instituto de Biopatología y Medicina Regenerativa (IBIMER); Departamento de Anatomía y Embriología Humana, Facultad de Medicina, Avenida de Madrid s/n, 18071 Granada (Spain).*

[c]*Departamento de Ciencias de la Salud, Facultad de Ciencias Experimentales y de la Salud, Paraje de las Lagunillas s/n, 23071 Jaén (Spain).*

[1]*These authors contributed equally to this work*

Abstract

As leads we took several benzo-fused seven- and six-membered scaffolds linked to the pyrimidine or purine moieties with notable anti-proliferative activity against human breast, colon and melanoma cancerous cell lines. We then decided to maintain the double-ringed nitrogenous bases and change the other components to the ethyl acetate moiety. This way six purine and two 5-fluorouracil derivatives were obtained and evaluated against the MCF-7, HCT-116, A375 and G361 cancer cell lines. Two QSARs are obtained between the anti-proliferative IC_{50} values for compounds **26-33** and the clog *P* against the melanoma cell lines A375 and G361. Our results show that two of the analogues [ethyl 2-(2,6-dichloro-9*H*- or 7*H*-purine-9- or 7-yl)acetates (**30** and **33**, respectively)] are potent citotoxic agents against all the tumour cell lines assayed, showing single-digit micromolar IC_{50} values. This exemplifies the potential of our previously reported purine compounds to qualify as lead structures for medicinal chemistry campaigns, affording simplified analogues easy to synthesize and with a noteworthy bioactivity. The selective activity of **30** and **33** against the melanoma cell line A375, via apoptosis, supposes a great advantage for a future therapeutic use.

Keywords: Anti-tumour compounds; Apoptosis; 5-Fluorouracil; Breast cancer; Colon cancer; Melanoma; Purines.

*Corresponding author: J.M. Campos. Phone: +34-958243850; Fax: +34-958243845; E-mail: jmcampos@ugr.es

Abbreviations: American Type Culture Collection: ATCC; Dulbecco's modified Eagle's medium: DMEM; 5-Fluorouracil: 5-FU; Phosphate Buffered Saline: PBS; Quantitative structure activity relationship: QSAR; Sodium Dichloroacetate: DCA; Sulforhodamine-B: SRB.

1. Introduction

Breast cancer is the first cause of death by neoplasia among women of industrialized countries and represents nearly 25% of non-accidental deaths of women between 35 and 54 years of age [1]. The frequency of breast cancer increases with age up to the menopause and subsequently continues to rise but more slowly [2]. Conventional cancer chemotherapy blocks cell division but lacks selectivity for oncogenic cells which can result in serious cytotoxic side effects for the patient. The key to specificity in cancer chemotherapy may be found in the pharmacological targeting of specific molecules avoiding cytotoxicity against normal cells [3].

Metastatic melanoma is a disease with limited treatment options and a poor prognosis. Malignant melanoma is the most aggressive form of skin cancer with increasing incidence over the past years [4]. Metastatic melanoma has a short median survival and is responsible for most skin cancer deaths [5]. Often

melanomas are characterized by resistance to cytotoxic agents because of the inactivation of apoptotic pathways [6].

Colorectal cancer (CRC) is a common disease that results in significant worldwide morbidity and mortality. CRC is the second leading cause of global cancer mortality, and accounts for over 600,000 deaths annually [7].

Having previously reported the synthesis and anticancer activities of cyclic 5-fluorouracil (5-FU) *O,N*-acetalic compounds (**1**), we changed 5-FU for uracil (**2**), with the aim of finding an anti-proliferative agent endowed with a new mechanism of action. Following our ongoing Anticancer Drug Programme we planned the synthesis of compounds bearing a pyrimidine base, and also the oxygen atom at position 1 of the seven-membered cycle was replaced by its isosteric sulfur atom (**3**, **4**) and its oxidized states. Later on, the pyrimidine base was substituted for the purine one with the objective of increasing both the lipophilicity and the structural diversity of the target molecules (**5-19**). Structures were designed in which both structural entities (such as the benzoheterocyclic ring and the purine base) were linked through a methylene linker (**20-25**). A series of (*RS*)-9-(2,3-dihydro-1,4-benzoxathiin-3-ylmethyl)-9*H*-purine derivatives (**20-22**) were obtained and the anticancer activity for the most active compounds was correlated with their capability to induce apoptosis. In order to complete a SAR study, a series of (*RS*)-6-substituted-7- or 9-(1,2,3,5-tetrahydro-4,1-benzoxazepine-3-yl)-7*H*- or 9*H*-purines (**23-25**) was prepared [8] (Chart 1).

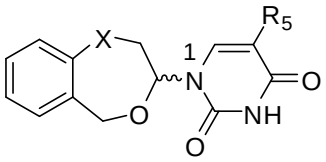

1 X = O; R_5 = F
2 X = O; R_5 = H
3 X = S; R_5 = F
4 X = S; R_5 = H

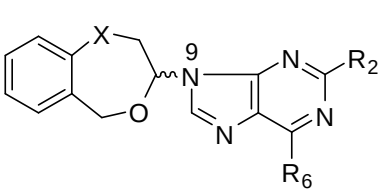

5 X = O; R_2 = H; R_6 = Cl
6 X = O; R_2 = H; R_6 = I
7 X = O; R_2 = R_6 = Cl
8 X = S; R_2 = H; R_6 = Cl
9 X = SO_2; R_2 = H; R_6 = Cl

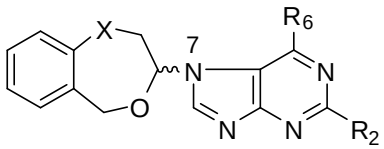

10 X = O; R_2 = H; R_6 = Cl
11 X = O; R_2 = H; R_6 = Cl
12 X = O; R_2 = R_6 = Cl
13 X = S; R_2 = H; R_6 = Cl
14 X = SO_2; R_2 = H; R_6 = Cl

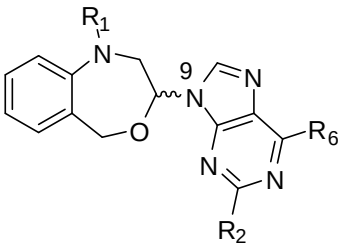

15 R_1 = SO_2-C_6H_4-*p*NO_2; R_2 = H; R_6 = Cl
16 R_1 = SO_2-C_6H_4-*p*NO_2; R_2 = R_6 = Cl
17 R_1 = Fmoc, R_6 = Cl

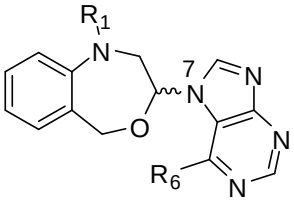

18 R_1 = SO_2-C_6H_4-*p*NO_2, R_6 = Cl
19 R_1 = Fmoc, R_6 = Cl

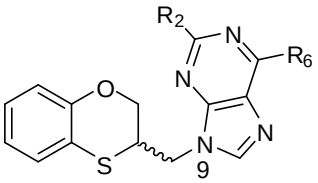

20 R_2 = H, R_6 = Cl
21 R_2 = H; R_6 = Br
22 R_2 = Cl; R_6 = Cl

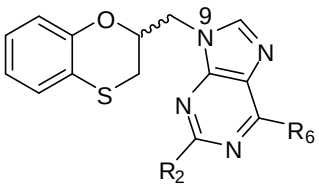

23 R_2 = H, R_6 = Cl
24 R_2 = H; R_6 = Br
25 R_2 = R_6 = Cl

Chart 1.

Compound **16** presents an IC_{50} of 0.166 μM against the human cancerous cell line MDA-MB-231. Compound **16** was the most selective against the human breast adenocarcinoma MCF-7 and MDA-MB-231 cancer cell lines (Therapeutic Indexes = 5.1 and 11.0, respectively) in relation to the normal MCF-10A. (*RS*)-**16** was resolved into its enantiomers. Both homochiral forms are equally potent, but more so than the corresponding racemic mixture [9].

The Mitsunobu reaction products were studied between (*RS*)-2,3-dihydro-1,4-benzoxathiin-3-methanol and the heterocyclic bases, 6-chloro-, 6-bromo- and 2,6-dichloro-purines under microwave-assisted conditions. The most active compounds against the human breast cancer cell line MCF-7 were **24**, and **25** with IC_{50} = 4.87 ± 0.02 μM and 2.75 ± 0.03, respectively [10].

The small molecule sodium dichloroacetate (DCA) inhibits the growth of C6 glioma tumours in both C6 brain tumour-bearing rats and C6 tumour-bearing nude mice [11]. Sánchez et al. have reported that the combination of DCA with bortezomib significantly extends the survival of myeloma-bearing mice over bortezomib alone and provides preclinical support for the use of this drug combination against myeloma [12].

We took the benzo-fused seven- and six-membered scaffolds linked to the pyrimidine or purine moieties **1-25** (Chart 1) as leader compounds, and decided to maintain the double-ringed nitrogenous bases and, as a first approach, connect the other components to the ethyl acetate (drastic molecular pruning) rest, which is related to DCA. Such a very simple reasoning has guided us in spite of a remote resemblance to the model structures. Should compounds **26**-**33** show notorious anti-proliferative activity, the simplicity of their preparation and the use of ordinary chemistry militate in their favour, although is not always accepted with enthusiasm by organic chemists. In this communication we report the synthesis and anti-proliferative activity against the human breast cancer cell line MCF-7, the human colon carcinoma cell line HCT-116, and two human melanoma cell lines such as A375 and G361 of two 5-FU derivatives (**26, 27**), and six purine scaffolds (**28**-**33**) (Chart 2).

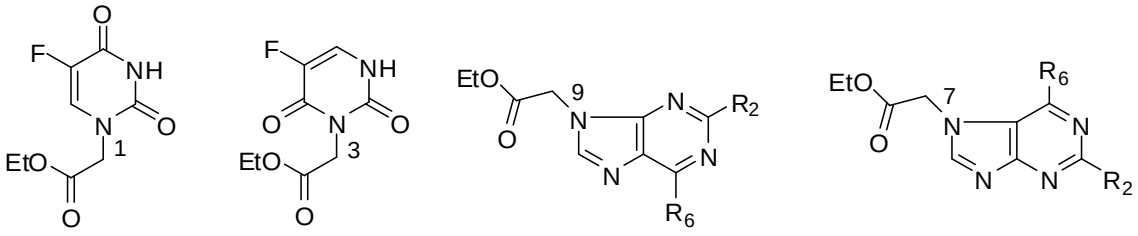

26 **27**

28 R_2 = H; R_6 = Cl
29 R_2 = H; R_6 = Br
30 R_2 = R_6 = Cl

31 R_2 = H; R_6 = Cl
32 R_2 = H; R_6 = Br
33 R_2 = R_6 = Cl

Chart 2.

2. Results and discussion

2.1. Chemistry

Compounds **26**-**33** were obtained as shown in Scheme 2(Chart 3).

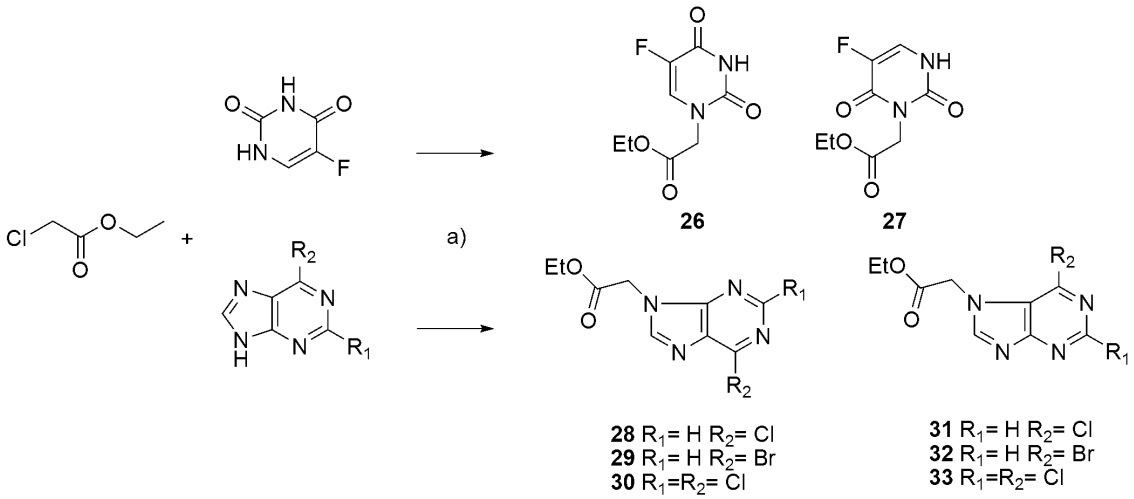

26 **27**

28 R_1= H R_2= Cl
29 R_1= H R_2= Br
30 R_1=R_2= Cl

31 R_1= H R_2= Cl
32 R_1= H R_2= Br
33 R_1=R_2= Cl

Scheme 2 (Chart 3?). *Reagents and conditions*: a) Et_3N, H_2O, 105 °C, MW, 8 min (13 % for **26**, 6 % for **27**, 24 % for **28**, 28 % for **29**, 40 % for **30**, 12 % for **31**, 9 % for **32**, 15 % for **33**).

Nucleophilic substitution assisted by microwave irradiation of ethyl chloroacetate using water as solvent and Et_3N as a base reagent afforded compounds **26**-**33**. This rapid, convenient and green protocol was previously

reported for the synthesis of **28** and **30** [13]. Whereas the authors only isolated *N*-9 isomers (**28** and **30**), we obtained *N*-9 and *N*-7 isomers in each reaction (**28** and **31**, **30** and **33**, respectively). (With the same reaction conditions,) we also prepared the synthesis of the bromopurine and 5-FU derivatives obtaining the *N*-9 and *N*-7 bromopurine isomers (**29** and **32**) and the *N*-1 and *N*-3 5-FU isomers (**26** and **27**). Compound **26** was previously reported [14], although in a non-easily accessible journal. The synthesis of its *N*-3 5-FU isomer (**27**) is described in another Chinese journal, in which its melting point is not provided [15].

2.2. Spectroscopic analysis

Compounds **26**-**33** have been identified by NMR-spectroscopy and high resolution mass spectroscopy. HSQC and HMBC studies were employed for the unequivocally identification of each atom of H and C. The discrimination between the *N*-9 and *N*-7 substituted purine derivatives (**28**-**33**) relies on the observation of the 1,3-relationship between the hydrogen atoms of the carbon linked to the purine and the quaternary carbons of the purine moiety: $C4_{pur}$ and $C5_{pur}$ in the HMBC spectrum (Figure 1). While these hydrogen atoms are correlated with $C4_{pur}$ in the *N*-9 regioisomers, they are correlated with $C5_{pur}$ in the *N*-7 regioisomers (Scheme 3).

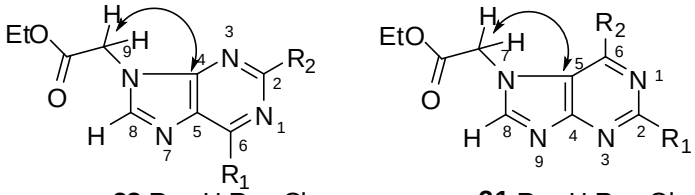

28 R_1= H R_2= Cl
29 R_1= H R_2= Br
30 R_1=R_2= Cl

31 R_1= H R_2= Cl
32 R_1= H R_2= Br
33 R_1=R_2= Cl

Scheme 3. The HMBC interactions that discriminate *N*-9 (**28**-**30**) and *N*-7 (**31**-**33**) purine regioisomers.

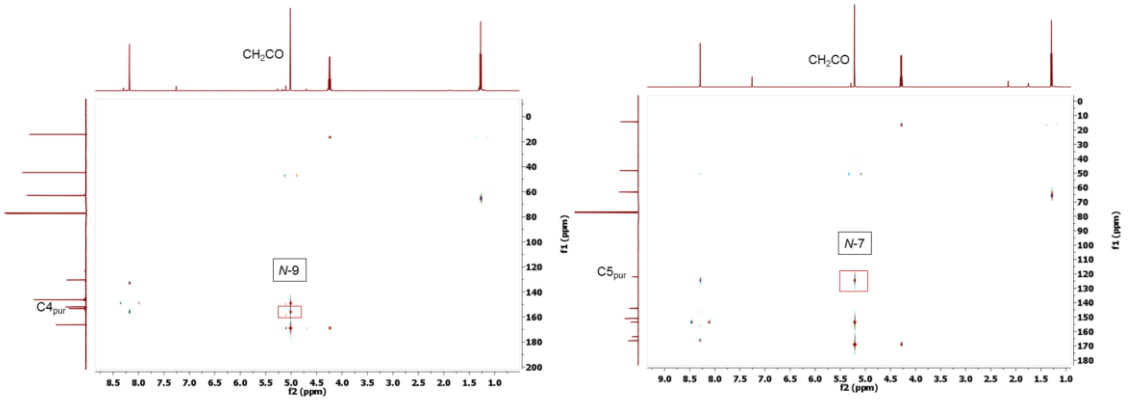

Figure 1. The HMBC spectrum of the *N*-9 (**30**) and *N*-7 (**33**) 2,6-dichloropurine isomers.

In the 5-FU derivatives, the identification of the *N*-1 isomer (**26**) relies on the observation of the 1,3-connection between the hydrogen atoms of the carbon linked to the 5-FU and the sole tertiary carbon of the 5-FU moiety ($C6_{5FU}$) and the opposite connection: $H6_{5FU}$ and the carbon linked to the 5-FU (Scheme 4) in the HMBC spectrum (Figure 2). These correlations do not exist in its isomer *N*-3 (**27**). The correlation in **27** appears between the hydrogen atoms of the carbon linked to the 5-FU and $C4_{5FU}$.

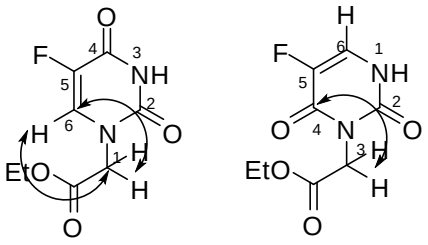

26 **27**

Scheme 4. The HMBC interactions that discriminate *N*-1 (**26**) and *N*-3 (**27**) 5-FU derivatives.

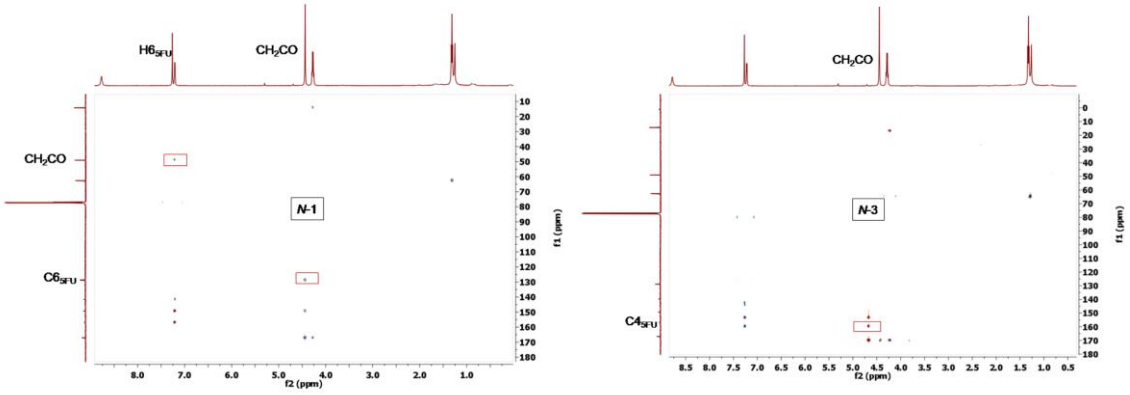

Figure 2. The HMBC spectrum of the *N*-1 (**26**) and *N*-3 (**27**) 5-fluoroacil isomers.

2.3. Biological activities

Table 1 shows the anti-proliferative activities against the MCF-7, HCT-116, A375 and G361 cancerous cell lines for the target compounds. As a rule of thumb, the following can be stated: (a) The 2,6-dichloropurine derivatives (**30**, **33**) are the most active compounds showing single-digit micromolar IC_{50} values against all the assayed cell lines, the *N*-9 derivative (**30**) eliciting improved activities in all cancerous cell lines than its *N*-7 regioisomer (**33**); (b) In general, the *N*-9 purine derivatives present an augmented activity than that of their *N*-7

regioisomers except in the case of the 6-chloropurines (**28** and **29**), in which this tendency is reversed against A375, and G361: both regioisomers are equally potent in inhibiting both melanoma cancer cell growth; (c) The 5-FU derivatives evidence intermediate potencies (IC_{50} ≈ 22 and 50 μM), being the *N*-1 isomer (**26**) more active than *N*-3 (**27**) against MCF-7 and A375, except in the case of HCT-116 and G361 cell lines.

A quick look at the IC_{50} values suggests that a correlation with the lipophilicity of the target compounds may exist, and we therefore decided to find the corresponding QSAR equations. Used in its logarithmic form (log *P*) the octanol-water partition coefficient is the most widely accepted measure of lipophilicity. Fragmental methods make it possible to create data banks and to perform log *P* calculations by computer.

Correlations 1 and 2 show the anti-proliferative activities of the targeted compounds against the melanoma cell line A375 and the clog *P* values of **26-33**. Such clog *P* values reported in Table 1 were calculated using the PALLAS programme [17].

$$p(IC_{50})_{A375} = 4.40\ (\pm 0.12) + 0.85\ (\pm 0.15)\ \text{clog}\ P \qquad (1)$$

$n = 8$, $r = 0.920$, $s = 0.224$, $F_{1,5} = 32.96$, $p < 0.005$

where $p(IC_{50})_{A375} = -\log (IC_{50})_{A375}$, bearing in mind that the higher the value of $p(IC_{50})_{A375}$ the more potent is the compound, *n* is the number of compounds, *r* is the correlation coefficient, *s* is the standard deviation, data within parentheses are standard errors of estimate, and $F_{1,5}$ is the Fisher test ($p < 0.005$).

Eq 2 shows the anti-proliferative activity of the targeted compounds against the G361 cell line:

$$p(IC_{50})_{G361} = 4.55\ (\pm\ 0.08) + 0.55\ (\pm\ 0.10)\ \text{clog}\ P \qquad (2)$$

$n = 8$, $r = 0.920$, $s = 0.159$, $F_{1,5} = 27.12$, $p < 0.005$

No correlation is obtained for the anti-proliferative activity of **26**-**33** and their clog *P* values ($r = 0.631$ against MCF-7, and $r = 0.353$ against HCT-116).

Table 1. Anti-proliferative activities[a] for compounds **26**-**33** against the cancerous cell lines MCF-7, HCT-116, A375 and G361.

Comp	IC_{50} (μM) MCF-7	IC_{50} (μM) HCT-116	IC_{50} (μM) A375	IC_{50} (μM) G361	clog*P*[b]
26	25.2 ± 0.03	24.6 ± 0.01	38.4 ± 0.06	29.0 ± 0.01	-0.07 ± 0.20
27	30.5 ± 0.03	22.6 ± 0.01	50.9 ± 0.13	25.4 ± 0.01	-0.27 ± 0.19
28	35.1 ± 0.03	5.27 ± 0.04	18.9 ± 0.09	21.4 ± 0.01	0.49 ± 0.15
31	49.8 ± 0.03	68.0 ± 0.04	14.5 ± 0.12	21.4 ± 0.01	0.49± 0.15
29	14.1 ± 0.06	23.5 ± 0.04	13.4 ± 0.03	15.8 ± 0.01	0.56 ± 0.14
32	20.2 ± 0.06	55.7 ± 0.04	26.7 ± 0.01	18.3 ± 0.01	0.51 ± 0.14
30	3.93 ± 0.04	6.20 ± 0.05	1.18 ± 0.03	3.06 ± 0.01	1.34 ± 0.15
33	5.63 ± 0.03	6.36 ± 0.06	4.98 ± 0.07	5.67 ± 0.01	1.32 ± 0.15

[a]All experiments were conducted in duplicate and gave similar results. The data are means ± SEM of three independent determinations.

[b]Pallas 3.8.1.1 CompuDrug Chemistry Ltd. Copyright (c) 1994, 2006.

The use of cell-cycle-specific treatments in cancer therapy has greatly benefited from the major advances that have been recently made in the identification of the molecular actors regulating the cell cycle and from the better understanding of the connections between cell cycle and apoptosis [18]. To study the mechanisms of the anti-tumour activity of the most active compounds (**30** and **33**), the effects on the cell cycle distribution and apoptosis were analysed by flow cytometry (Tables 2, 3 and 4). For this purpose we used the MCF-7, HCT-116 and A375 cell lines as representatives for breast, colon and melanoma tumours, respectively. The A375 melanoma cell line was selected because of its higher metastatic phenotype in comparison with G361 [19]. MCF-7 cells treated for 24 h with **30** and **33** did not show significant differences in the cell cycle progression compared with DMSO-treated control cells. We found a slight cell cycle arrest in the G_2/M and S-phases induced by **30** (54.63 ± 1.18) and **33** (18.27 ± 0.79), respectively (Table 2). In the HCT-116 and A375 treated cells, **30** did not modify the cell cycle profile and **33** provoked a G_2/M cell cycle arrest (28.47 ± 0.07) at the expense of the G_0/G_1-phase (33.58 ± 1.90) in the colon cancer cells and accumulated the A375 melanoma cells in the G_0/G_1-phase (70.55 ± 1.47) at the expense of both G_2/M and S phases (20.10 ± 0.75 and 9.34 ± 0.62, respectively) (Tables 3 and 4). Previously, we have demonstrated that potent anti-tumour drugs did not modify the cell cycle in comparison with control cells, due to a translational block and consequently inhibition of the protein synthesis by the activation and phosphorylation of the initiation factor eIF2α [10].

Table 2. Cell cycle distribution and apoptosis induction in the human breast MCF-7 cancer cell line after treatment for 24 h for the two most active compounds **30** and **33** as anti-proliferative agents.

Compound	**Cell cycle**[a,b]			**Apoptosis**[a,b,c]
	G_0/G_1	S	G_2/M	
Control	34.58 ± 0.09	14.50 ± 1.06	50.91 ± 1.15	10.80 ± 0.85
30	28.17 ± 1.37	15.39 ± 0.68	54.63 ± 1.18	20.53 ± 0.91
33	34.54 ± 0.08	18.27 ± 0.79	47.19 ± 0.89	24.10 ±4.37

[a]Determined by flow cytometry [18].

[b] All experiments were conducted in triplicate and gave similar results. The data are means ± SEM of three independent determinations.

[c]Apoptosis was determined using an Annexin V-based assay [18]. The data indicate the percentage of cells undergoing apoptosis in each sample.

Table 3. Cell cycle distribution and apoptosis induction in the HCT-116 colon cancer cell line after treatment for 24 h for the two most active compounds **30** and **33** as anti-proliferative agents.

Compound	**Cell cycle**[a,b]			**Apoptosis**[a,b,c]
	G_0/G_1	S	G_2/M	
Control	44.70 ± 0.38	38.26 ± 1.40	17.02 ± 1.40	7.27 ± 1.57
30	45.93 ± 1.11	36.75 ± 0.70	17.31 ± 0.44	20.20 ± 3.18
33	33.58 ± 1.90	37.93 ± 1.92	28.47 ± 0.07	17.03 ± 1.00

[a]Determined by flow cytometry [18].

[b]All experiments were conducted in triplicate and gave similar results. The data are means ± SEM of three independent determinations.

[c]Apoptosis was determined using an Annexin V-based assay [18]. The data indicate the percentage of cells undergoing apoptosis in each sample.

Table 4. Cell cycle distribution and apoptosis induction in the A375 colon cancer cell line after treatment for 24 h for the two most active compounds **30** and **33** as anti-proliferative agents.

Compound	**Cell cycle**[a,b]			**Apoptosis**[a,b,c]
	G_0/G_1	S	G_2/M	
Control	57.97 ± 0.93	29.60 ± 0.78	12.42 ± 0.70	6.83 ± 0.40
30	58.48 ± 1.03	28.78 ± 0.26	12.73 ± 0.77	35.37 ± 0.47
33	70.55 ± 1.47	20.10 ± 0.75	9.34 ± 0.62	27.13 ± 3.07

[a]Determined by flow cytometry [18].

[b]All experiments were conducted in triplicate and gave similar results. The data are means ± SEM of three independent determinations.

[c]Apoptosis was determined using an Annexin V-based assay [18]. The data indicate the percentage of cells undergoing apoptosis in each sample.

Apoptotic defects in cancer cells are the primary obstacle that limits the therapeutic efficacy of anticancer agents, and hence the development of novel agents targeting programmed cell death pathways has become an imperative mission for clinical research [20,21]. Although both compounds showed different cell cycle profiles that were dependent upon the cell line studied, however, **30** and **33** at 24 h induced high levels of apoptosis in all cancer cells in comparison with DMSO-treated cell cultures (Tables 2, 3 and 4). This apoptosis was induced even in the MCF-7 breast cancer cells that have shown deficiency in

the caspase-activation mechanisms [22]. Interestingly, **30** was the most apoptotic compound against the A375 melanoma cell line (35.37 ± 0.47), where no modification in the cell cycle were found. This effect could be explained by a preferentially apoptotic mechanism of action. Moreover, the fact that **33** gathered cells at G_2/M and G_0/G_1 phases respectively in the colon and melanoma cancer cells accompanied by high levels of programmed death cell indicates that this compounds has different cytotoxic effects on each tumour cell type.

3. Conclusion

The anti-proliferative potential of the target molecules is reported against four human cancerous cell lines. Two QSARs are obtained between the anti-proliferative IC_{50} values for compounds **26-33** and the clog *P* against the melanoma cell lines A375 and G361. Using our purine derivatives as lead structures, we have obtained a simplified analogue with a remarkable bioactivity. The most active compounds are always **30** and **33** and the results indicate that the anti-proliferative activity of **33** is correlated with its ability to induce apoptosis against the human melanoma cell line A375. The mechanism through which molecules **30** and **33** elicit their effects is currently being elucidated.

4. Experimental protocols

4.1. Chemistry

Melting points were taken in open capillaries on an Electrothermal melting point apparatus and are uncorrected. Analytical thin layer chromatography was performed using Merck Kieselgel 60 F254 aluminum sheets, the spots being developed with UV light (λ = 254 nm). All evaporation was carried out in vacuo with a Büchi rotary evaporator and the pressure controlled by a Vacuubrand CVCII apparatus. For flash chromatography, Merck silica gel 60 with a particle size of 0.040-0.063 mm (230-400 mesh ASTM) was used. Nuclear magnetic resonance spectra have been carried out at the Centro de Instrumentación Científica/Universidad de Granada, and recorded on a 300 MHz ^{1}H and 75 MHz ^{13}CNMR Varian Inova-TM spectrometers at ambient temperature. Chemical shifts (δ) are quoted in parts per million (ppm) and are referenced to the residual solvent peak. Signals are designated as follows: s, singlet; d, doublet; t, triplet; pst, pseudo-triplet; q, quartet. High-resolution Nano-Assisted Laser Desorption/Ionization (NALDI-TOF) or Electrospray Ionization (ESITOF) mass spectra were carried out on a Bruker Autoflex or a Waters LCT Premier Mass Spectrometer, respectively. Small scale microwave-assisted synthesis was carried out in an Initiator 2.0 single-mode microwave instrument producing controlled irradiation at 2.450 GHz (Biotage AB, Uppsala). Reaction time refers to hold time at 105 ºC, not to total irradiation time. The temperature was measured with an IR sensor outside the reaction vessel. Anhydrous THF was purchased from VWR International Eurolab. Anhydrous conditions were

performed under argon. 6-Chloropurine, 6-bromopurine and 2,6-dichloropurine were purchased from Aldrich.

4.1.1. General procedure for the Microwave-assisted synthesis of 26-33

Ethyl chloroacetate (6 mmol) was added drop wise to a mixture of TEA (4 mmol) and the corresponding purine derivative or 5-FU (2 mmol) in water (5 mL). The microwave vial was sealed and irradiated at 105 ºC for 8 min. After completion of irradiation time and cooling to room temperature through rapid pressurized air supply gas-jet, the resulting mixture was extracted with CH_2Cl_2 (3 × 50 mL) and the organic phase was dried ($MgSO_4$). The solvent was evaporated and the residue was purified by flash chromatography using CH_2Cl_2/CH_3OH (10/0.1) as eluent.

4.1.1.1. 5-Fluoro-1-(ethoxycarbonylmethyl)-3H-pyrimidine-2,4-dione (26). White solid (57 mg, 13 %); mp: 165-166 ºC (lit[14] 164-165 ºC). ^{1}H NMR (300 MHz, $CDCl_3$): δ= 8.83 (s, 1H, H1), 7.21 (d, *J*= 5.3 Hz, 1H, H6), 4.43 (s, 2H, CH_2CO), 4.27 (q, *J* = 7.1 Hz, 2H, CH_2O), 1.31 (t, *J*= 7.1 Hz, 3H, CH_3). ^{13}C NMR (75 MHz, $CDCl_3$): δ= 167.09 (CO), 156.87 (C4), 149.31 (C2), 141.60 (C5), 128.86 (C6), 62.67 (CH_2O), 49.02 (CH_2CO), 14.24 (CH_3). HRMS m/z $[M+H]^+$ calcd for $C_8H_{10}FN_2O_4$: 217.0546, found: 217.0546. Anal. Calc. for $C_8H_9FN_2O_4$: C, 44.45; H, 4.20; N, 12.96. Found: C, 44.21; H, 4.39; N, 13.01.

4.1.1.2. 5-Fluoro-3-(ethoxycarbonylmethyl)-1H-pyrimidine-2,4-dione (27). Light orange solid (26 mg, 6 %); mp: 131-132 ºC. ^{1}H NMR (300 MHz, $CDCl_3$): δ= 9.26 (s, 1H, H1), 7.29 (pst, 1H, H6), 4.68 (s, 2H, CH_2CO), 4.24 (q, *J* = 7.1 Hz, 2H, CH_2O), 1.30 (t, *J* = 7.1 Hz, 3H, CH_3). ^{13}C NMR (75 MHz, $CDCl_3$): δ= 167.09 (CO), 156.77 (C4), 149.59 (C2), 139.70 (C5), 128.59 (C6), 62.67 (CH_2O), 49.07

(CH_2CO), 14.24 (CH_3). HRMS m/z $[M+H]^+$ calcd for $C_8H_{10}FN_2O_4$: 217.0546, found: 217.0546. Anal. Calc. for $C_8H_9FN_2O_4$: C, 44.45; H, 4.20; N, 12.96. Found: C, 44.21; H, 4.59; N, 12.63.

4.1.1.3. 6-Chloro-9-(ethoxycarbonylmethyl)-9H-purine (28). White solid (117 mg, 24 %); mp: 97-98 ºC (lit[16] 96-98 ºC). ^{1}H NMR (300 MHz, $CDCl_3$): δ= 8.74 (s, 1H, H2), 8.20 (s, 1H, H8), 5.05 (s, 2H, CH_2CO), 4.27 (q, *J* = 7.1 Hz, 2H, CH_2O), 1.29 (t, *J* = 7.1 Hz, 3H, CH_3). ^{13}C NMR (75 MHz, $CDCl_3$): δ= 166.56 (CO), 152.37 (C2), 152.03 (C4), 151.39 (C6), 145.58 (C8), 131.33 (C5), 62.82 (CH_2O), 44.69 (CH_2CO), 14.20 (CH_3). HRMS m/z $[M+H]^+$ calcd for $C_9H_{10}ClN_4O_2$: 241.0414, found: 241.0488. Anal. Calc. for $C_9H_9ClN_4O_2$: C, 44.92; H, 3.77; N, 23.28. Found: C, 44.99; H, 3.59; S, 23.39.

4.1.1.4. 6-Chloro-7-(ethoxycarbonylmethyl)-7H-purine (31). White solid (59 mg, 12 %); mp: 122-123 ºC. ^{1}H NMR (300 MHz, $CDCl_3$): δ= 8.87 (s, 1H, H2), 8.28 (s, 1H, H8), 5.23 (s, 2H, CH_2CO), 4.27 (q, *J* = 7.1 Hz, 2H, CH_2O), 1.27 (t, *J* = 7.1 Hz, 3H, CH_3). ^{13}C NMR (75 MHz, $CDCl_3$): δ= 166.76 (CO), 162.00 (C4), 152.81 (C2), 149.72 (C6), 143.16 (C8), 122.80 (C5), 62.90 (CH_2O), 48.19 (CH_2CO), 14.17 (CH_3). HRMS m/z $[M+H]^+$ calcd for $C_9H_{10}ClN_4O_2$: 241.0414, found: 241.0487. Anal. Calc. For $C_9H_9ClN_4O_2$: C, 44.92; H, 3.77; N, 23.28. Found: C, 45.21; H, 3.59; N, 23.42.

4.1.1.5. 6-Bromo-9-(ethoxycarbonylmethyl)-9H-purine (29). White solid (157 mg, 28 %); mp: 104-105 ºC. ^{1}H NMR (300 MHz, $CDCl_3$): δ= 8.71 (s, 1H, H2), 8.23 (s, 1H, H8), 5.05 (s, 2H, CH_2CO), 4.28 (q, *J* = 7.1 Hz, 2H, CH_2O), 1.30 (t, *J*= 7.2 Hz, 3H, CH_3). ^{13}C NMR (75 MHz, $CDCl_3$): δ= 166.52 (CO), 152.36 (C2), 150.80 (C4), 145.53 (C8), 143.46 (C6), 133.89 (C5), 62.85 (CH_2O), 44.75

(CH_2CO), 14.21 (CH_3). HRMS m/z $[M+H]^+$ calcd for $C_9H_{10}BrN_4O_2$: 284.9909, found: 284.9910. Anal. Calc. for $C_9H_9BrN_4O_2$: C, 37.92; H, 3.18; N, 19.65. Found: C, 37.72; H, 3.49; N, 19.38.

4.1.1.6. 6-Bromo-7-(ethoxycarbonylmethyl)-7H-purine (32). Yellow syrup (50 mg, 9 %). ^{1}H NMR (300 MHz, $CDCl_3$): δ= 8.90 (s, 1H, H2), 8.65 (s, 1H, H8), 5.32 (s, 2H, CH_2CO), 4.29 (q, *J* = 7.1 Hz, 2H, CH_2O), 1.29 (t, *J* = 7.1 Hz, 3H, CH_3). ^{13}C NMR (75 MHz, $CDCl_3$): δ= 166.67 (CO), 159.41 (C4), 152.99 (C2), 149.77 (C8), 133.93 (C6), 122.69 (C5), 63.06 (CH_2O), 48.29 (CH_2CO), 14.21 (CH_3). HRMS m/z $[M+H]^+$ calcd for $C_9H_{10}BrN_4O_2$: 284.9909, found: 284.9991. Anal. Calc. For $C_9H_9BrN_4O_2$: C, 37.92; H, 3.18; N, 19.65. Found: C, 37.64; H, 3.42; N, 19.33.

4.1.1.7. 2,6-Dichloro-9-(ethoxycarbonylmethyl)-9H-purine (30). White solid (218 mg, 40 %); mp: 120-121 ºC (lit[13] 112-113 ºC). ^{1}H NMR (300 MHz, $CDCl_3$): δ= 8.18 (s, 1H, H8), 5.02 (s, 2H, CH_2CO), 4.24 (q, *J* = 7.1 Hz, 2H, CH_2O), 1.28 (t, *J*= 7.2 Hz, 3H, CH_3). ^{13}C NMR (75 MHz, $CDCl_3$): δ= 166.25 (CO), 153.30 (C6), 153.26 (C4), 151.95 (C2), 146.33 (C8), 130.39 (C5), 62.90 (CH_2O), 44.70 (CH_2CO), 14.10 (CH_3). HRMS m/z $[M+H]^+$ calcd for $C_9H_9Cl_2N_4O_2$: 275.0024, found: 275.0096. Anal. Calc. for $C_9H_8Cl_2N_4O_2$: C, 39.29; H, 2.93; N, 20.37. Found: C, 39.01; H, 2.63; N, 20.09.

4.1.1.8. 2,6-Dichloro-7-(ethoxycarbonylmethyl)-7H-purine (33). Yellow syrup (82 mg, 15 %). ^{1}H NMR (300 MHz, $CDCl_3$): δ= 8.29 (s, 1H, H8), 5.22 (s, 2H, CH_2CO), 4.29 (q, *J* = 7.1 Hz, 2H, CH_2O), 1.29 (t, *J* = 7.1 Hz, 3H, CH_3). ^{13}C NMR (75 MHz, $CDCl_3$): δ= 166.49 (CO), 163.61 (C4), 153.53 (C6), 152.00 (C8), 143.90(C2), 122.05 (C5), 63.11 (CH_2O), 48.25 (CH_2CO), 14.21 (CH_3). HRMS

m/z $[M+H]^+$ calcd for $C_9H_9Cl_2N_4O_2$: 275.0024, found: 274.0096. Anal. Calc. for $C_9H_8Cl_2N_4O_2$: C, 39.29; H, 2.93; N, 20.37. Found: C, 38.91; H, 2.64; N, 20.20.

4.2. Biology

4.2.1. Cell culture

MCF-7, HCT-116, A375 and G361 cells were grown at 37 ºC in an atmosphere containing 5 % CO2, with Dubelcco's modified Eagle Medium (DMEM) (Gibco, Grand Island, NY, USA) supplemented with 10 % heat-inactivated fetal bovine serum (FBS) (Gibco), 2 % L-glutamine, 2.7 % sodium bicarbonate, 1 % Hepes buffer, 40 mg/L gentamicin and 500 mg/L ampicillin.

4.2.2. Drug treatment

Compounds were dissolved in DMSO and stored at -20 ºC. For each experiment, the stock solutions were further diluted in medium to obtain the desired concentrations. The final solvent concentration in cell culture was ≤ 0.1 % v/v of DMSO, a concentration without any effect on cell replication. Parallel cultures of MCF-7, HCT-116, A375 and G361 cells in medium with DMSO were used as controls.

4.2.3. Proliferation assays

The effect of the compounds on cell viability was assessed using the sulforhodamine-B (SRB) colorimetric assay. Cells suspension (30×10^3 cells/well) were seeded onto 24-well plates and incubated for 24 h. The cells were then treated with different concentrations of drugs in their respective

culture medium and maintained with the treatment for 3 additional days. Thereafter, we used a Titertek Multiscan (Flow, Irvine, California) at 492 nm. We evaluated linearity of the SRB assay with a cell number for each cell stock before each cell growth experiment. The inhibitory concentration 50 (IC_{50}) values were calculated from semi-logarithmic dose-response curves by linear interpolation. All of the experiments were plated in triplicate wells and were carried out twice.

4.2.4. Cell cycle distribution analysis

The cells at 70 % confluence were treated with either DMSO alone or with concentrations of compounds **30** and **33** determined by their IC_{50} values. FACS analysis was performed after 24 h of treatment as described [18]. All experiments were performed in triplicate and yielded similar results.

4.2.5. Apoptosis detection by staining with annexin V-FITC and propidium iodide

The annexin V-FITC apoptosis detection kit I (Pharmingen, San Diego, CA, USA) was used to detect apoptosis by flow cytometry according to Marchal et al. [18]. Apoptosis induction in the MCF-7, HCT-116 and A375 human cancer cell lines after treatment for 24 h was determined for compounds **30** and **33** at doses of their corresponding IC_{50}. All experiments were performed in triplicate and yielded similar results.

4.2.6. Statistical analyses

All the quantitative data in the present study are reported as means ± standard derivation from at least three independent experiments. Two-way

ANOVA was used for grouped analysis of differences followed by Bonferroni post-tests.

Acknowledgments

We thank the Instituto de Salud Carlos III [Fondo de Investigación Sanitaria (FIS) through projects no. PI10/00592 and PI10/02295] and the ERDF (European Regional Development Fund) for financial supports.

References

[1] G. Ursin, L. Bernstein, M.C. Pike, BreastCancer in: Trends in cancer incidence and mortality. Cold Spring Habor Laboratory Press, Plain-view, New York, 1994.

[2] V.F. Guinee, T. Moller T, Breast carcinoma in young patients, Lancet 356 (2000) 1113.

[3] P. Workman, S.B. Kaye, Translating basic cancer research into new cancer therapeutics,Trends Molec. Med. 8 (2002) S1–S9.

[4] D.L. Cummins, J.M. Cummins, H. Pantle, M.A. Silverman, A.L. Leonard, A. Chanmugam, Cutaneous malignant melanoma, Mayo Clin. Proc. 81 (2006) 500-507.

[5] A. Jemal, R. Siegel, E. Ward, T. Murray, J. Xu, C. Smigal, M.J. Thun, Cancer statistics, 2006, CA Cancer J. Clin. 56 (2006), 106-130.

[6] V. Gray-Schopfer, C. Wellbrock, R. Marais, Melanoma biology and new targeted therapy, Nature 445 (2007) 851-857.

[7] A. Jemal, F. Bray, M.M. Center, J. Ferlay, E. Ward, D. Forman, Global cancer statistics. CA Cancer J. Clin. 61(2011) 69–90.

[8] M.C. Núñez, M. Díaz-Gavilán, A. Conejo-García, O. Cruz-López, M.A. Gallo, A. Espinosa, J.M. Campos, Design, Synthesis and Anticancer Activity against the MCF-7 Cell Line of Benzo-Fused 1,4-Dihetero Seven- and Six-Membered Tethered Pyrimidines and Purines, Curr. Med. Chem. 15 (2008) 2614-2631.

[9] L.C. López-Cara, A. Conejo-García, J.A. Marchal, G. Macchione, O. Cruz-López, H. Boulaiz, M.A. García, F. Rodríguez-Serrano,A. Ramírez, C. Cativiela, A.I. Jiménez, J.M. García-Ruiz, D. Choquesillo-Lazarte, A. Aránega, J.M. Campos, New (*RS*)-Benzoxazepin-Purines with Antitumour Activity: The Chiral Switch from (*RS*)-2,6-Dichloro-9-[1-(*p*-Nitrobenzenesulfonyl)-1,2,3,5-Tetrahydro-4,1-Benzoxazepin-3-yl]-9*H*-Purine, Eur. J. Med. Chem. 46 (2011) 249-258.

[10] A. Conejo-García, M.E. García-Rubiño, J.A. Marchal, M.C. Núñez, A. Ramírez, S. Cimino, M.A. García, A. Aránega, M.A. Gallo, J.M. Campos, Synthesis and Anticancer Activity of (*RS*)-9-(2,3-Dihydro-1,4-Benzoxaheteroin-2-ylmethyl)-9*H*-Purines, Eur. J. Med. Chem 46 (2011) 3795-3801.

[11] Y. Duan, X. Zhao, W. Ren, X. Wang, K.F. Yu, D. Li, X. Zhang, Q. Zhang, Antitumour activity of dichloroacetate on C6 glioma cell: in vitro and in vivo evaluation, OncoTargetsTher. 6 (2013) 189-198.

[12] W.Y. Sánchez, S.L. McGee, T. Connor, B. Mottram, A. Wilkinson, J.P. Whitehead, S. Vuckovic, L. Catley, Dichloroacetate inhibits aerobic glycolysis in multiple myeloma cells and increases sensitivity to bortezomib, Br. J. Cancer 108 (2013) 1624-1633.

[13] G. Qu, Z. Zhang, H. Guo, M. Geng, R. Xia, Microwave-Assisted Rapid and Regioselective Synthesis of *N*-(alkoxycarbonylmethyl) Nucleobases in Water, J. Braz. Chem. Soc. 18 (2007) 1061-1067.

[14] S. Xu, W. Zhang, Green synthesis of N1-[(ethoxycarbonyl)methyl]-5-fluorouracil under microwave irradiation conditions, Yingyong Huagong 37 (2008) 290-292.

[15] L. Xu, L. Weng, H. Zheng, Synthesis of 5-fluorouracil derivatives containing alkanoic acid, Sichuan Daxue Xuebao (Yixueban) 37 (2006) 644-646.

[16] Q. Zhang, G. Cheng, Y.-Z. Huang, G.-R. Qu, H.-Y. Niu, H.-M. Guo, Regioselective N9 alkylation of purine rings assisted by β-cyclodextrin, Tetrahedron 68 (2012) 7822-7826.

[17] PALLAS 3.8.1.1, a prediction tool of physicochemical parameters, is supplied by CompuDrug Chemistry, Ltd, PO Box, Rochester, NY 14692, USA.

[18] J.A. Marchal, H. Boulaiz, I. Suárez, E. Saniger, J. Campos, E. Carrillo, J. Prados, M.A. Gallo, A. Espinosa, A. Aránega, Growth inhibition, G1-arrest, and apoptosis in MCF-7 human breast cancer cells by novel highly lipophilic 5-fluorouracil derivatives, Invest. New Drug 22 (2004) 379-389.

[19] N. Ikoma, H. Yamazaki, Y. Abe, Y. Oida, Y. Ohnishi, H. Suemizu, H. Matsumoto, T. Matsuyama, Y. Ohta, A. Ozawa, Y. Ueyama, M. Nakamura, S100A4 expression with reduced E-cadherin expression predicts distant metastasis of human malignant melanoma cell lines in the NOD/SCID/gammaC null (NOG) mouse model, Oncol. Rep. 14 (2005) 633-637.

[20] B.S. Cummings, G.R. Kinsey, L.J. Bolchoz, R.G. Schnellmann, Identification of caspase-independent apoptosis in epithelial and cancer cells, J. Pharmacol. Exp. Ther. 310 (2004) 126-134.

[21] O. Caba, F. Rodríguez-Serrano, M. Díaz-Gavilán, A. Conejo-García, R. Ortiz, A. Martínez-Amat, P. Alvarez, M.A. Gallo, J.M. Campos, J.A. Marchal, A. Aránega, The selective cytotoxic activity in breast cancer cells by an anthranilic alcohol-derived acyclic 5-fluorouracil *O,N*-acetal is mediated by endoplasmic reticulum stress-induced apoptosis, Eur. J. Med. Chem. 50 (2012) 376-382.

[22] S. Kagawa, J. Gu, T. Honda, T.J. McDonnell, S.G. Swisher, J.A. Roth, B. Fang, Deficiency of caspase-3 in MCF7 cells blocks Bax-mediated nuclear fragmentation but not cell death, Clin. Cancer Res. 7 (2001) 1474-1480.

Captions to Charts

Chart 1. Benzo-fused seven-membered linked to pyrimidines (**1**-**4**), to purines (**5**-**19**), and benzo-fused six-membered rings linked to purines (**20**-**25**).

Chart 2. Target molecules under study in this communication: *N*-1 (**26**) and *N*-3 (**27**) 5-FU derivatives, *N*-9 (**28**-**30**) and *N*-7 (**31**-**33**) purine compounds.